Probing electron quadrupling order through ultrasound

Chris Halcrow,[1,*] Ilya Shipulin,[2] Federico Caglieris,[3,4,5] Yongwei Li,[6] Kunihiro Kihou,[7] Chul-Ho Lee,[7] Hans-Henning Klauss,[2] Sergei Zherlitsyn,[8] Vadim Grinenko,[6,†] and Egor Babaev[1,9,‡]

[1] *Department of Physics, KTH Royal Institute of Technology, SE-106 91 Stockholm, Sweden*
[2] *Institutefor Solid Stateand Materials Physics, Technische Universitat Dresden, D-01069 Dresden, Germany*
[3] *University of Genoa, Via Dodecaneso 33, 16146 Genoa, Italy*
[4] *Consiglio Nazionale delle Ricerche (CNR)-SPIN, Corso Perrone 24, 16152 Genova, Italy*
[5] *Leibniz Institute for Solid Stateand Materials Research, D-01069, Dresden, Germany*
[6] *Tsung-Dao Lee Institute & School of Physics and Astronomy, Shanghai Jiao Tong University, Shanghai 200240, China*
[7] *National Institute of Advanced Industrial Science and Technology (AIST), Tsukuba, Ibaraki 305-8568, Japan*
[8] *Hochfeld-Magnetlabor Dresden (HLD-EMFL), Helmholtz-Zentrum Dresden-Rossendorf, Bautzner Landstrasse 400, 01328 Dresden, Germany*
[9] *Wallenberg Initiative Materials Science for Sustainability*

Recent experiments have pointed to the formation of a new state of matter, the electron quadrupling condensate in $Ba_{1-x}K_xFe_2As_2$. The state spontaneously breaks time-reversal symmetry and is sandwiched between two critical points, separating it from the superconducting and normal metal states. The adjacent two critical points make acoustic effects a promising tool to study such states because of their sensitivity to symmetry-breaking transitions. We report a theory of the acoustic effects of systems with an electron quadrupling phase and new ultrasound velocity measurements of $Ba_{1-x}K_xFe_2As_2$ single crystals. The presented theory for the electron quadrupling state gives the same type of singularities that are observed in experiment.

I. INTRODUCTION

The electron quadrupling condensate is defined as a state whose order parameter is composed out of fermionic operators. In the case of $Ba_{1-x}K_xFe_2As_2$ the evidence was provided of the order parameter of the type$< c_{\sigma i}c_{\alpha i}c^\dagger_{\sigma j}c^\dagger_{\alpha j} >$, where α, σ are spin index and i, j are band indices. In contrast to superconductivity, formed by electron pairs, in $Ba_{1-x}K_xFe_2As_2$ this state spontaneously breaks time reversal symmetry (which is a double degenerate, i.e. Z_2 state); for early theory discussions see [1, 2]. The evidence for this state comes from calorimetric, transport, thermoelectric, and muon spin rotation probes which all suggest that it exists in a range of temperatures $T_c^{U(1)} < T < T_c^{Z_2}$ [3, 4]. Below $T_c^{U(1)}$ the system undergoes another phase transition to a superconducting state, signaling the onset of order at the level of electron pairs $< c_{\sigma i}c_{\alpha i} >$. A recent experiment [5] reported the creation of a related bosonic state. A mechanism describing the formation of fluctuations-induced composite electronic and bosonic orders has been well studied [1, 2, 6–14]. These models also predict vortices carrying a fraction of magnetic flux quantum and such vortices were recently observed in this compound [15]. While the experimental data gathered on $Ba_{1-x}K_xFe_2As_2$ at $x \approx 0.8$ reveals a set of unprecedented properties, most of the properties of this state remain unexplored.

One of the powerful methods to detect phase transitions, diagnose new states of matter and get insights into symmetries of the order parameters is ultrasound, which allows one to extract elastic constants of materials [3, 16–21]. In a conventional one-component superconductor, there is a discontinuous jump in the "compressional" ultrasound mode. This is because compressional strain always couples to the magnitude of the superconducting order parameter squared, $|\psi|^2$. In the other sound modes, there is a continuous change in the response due to higher-order coupling. The acoustic response is usually measured in a Pulse-Echo experiment or using Resonant Ultrasound Spectroscopy.

Complex ultrasound responses, such as discontinuous jumps in non-compressional sound modes, are predicted for unconventional superconductors [22] and are currently actively searched for in a variety of materials [20, 21, 23]. The responses can be used to get insight into the order parameter symmetry and structure. In a previous work, we observed an unprecedented type of ultrasound response in $Ba_{1-x}K_xFe_2As_2$ at doping $x = 0.81$ [3]. This is the same doping that all the other previously mentioned unusual responses occur and, hence, we will refer to it as "magic doping". Away from magic doping the ultrasound response is conventional. However, in the investigated sample with $x = 0.81$, there are two very distinct ultrasound singularities occurring at different temperatures. First, there is a feature in the "B_{1g}" shear mode in the quadrupling state, $T_c^{Z_2} < T < T_c^{U(1)}$. Second, there are jumps in the ultrasound response in both transverse and longitudinal modes at $T_c^{U(1)}$. As we will show, these features have strong theoretical implications and so deserve careful study and scrutiny.

There is no theory to date to explain the reported ul-

* chalcrow@kth.se
† vadim.grinenko@sjtu.edu.cn
‡ babaev@kth.se

trasound behavior and deduce whether it is related to the other observed probes [3, 4], both near the electron quadrupling transition at $T_c^{Z_2}$ and the subsequent transition from this state to the superconducting state at $T_c^{U(1)}$. In this work, we report both a new set of ultrasound measurements and a theory of ultrasound probes for the electron quadrupling state. We show below that the ultrasound data of $Ba_{1-x}K_xFe_2As_2$ with $x \approx 0.75 - 0.8$ supports the existence of the quandrupling state. Additionally, it contributes towards the problem of deciphering aspects of the momentum-space symmetries of pairing and quadrupling symmetries.

II. EXPERIMENTAL RESULTS

In our previous study, we observed that the $Ba_{1-x}K_xFe_2As_2$ ultrasound response depends on the doping level. Above ($x = 1$) and below ($x = 0.71$) the "magic" doping, there is only a definite jump in the sound velocity of the longitudinal acoustic mode at $T_c^{U(1)}$. This theoretically discontinuous jump takes place over several Kelvin; the broadening is likely due to sample inhomogeneity and imperfection of the mechanical contact between the transducers and thin ($\sim 10\mu$m) and long ($\sim$ 1mm) sample edge. The transverse ultrasound response changes continuously at $T_c^{U(1)}$, as expected for a conventional superconductor. The conventional character is consistent with the lack of indications of broken time reversal symmetry in muon and thermoelectric probes. At $x = 0.81$, the ultrasound data is unprecedented by having two unique features (Fig. ED6 of [3]). First, there is a clear linear signal in the "B_{1g}" shear mode, also known as the $(c_{11} - c_{22})/2$ mode, at the $\mathbb{Z}_2$ transition (detected via the appearance of spontaneous Nernst signal and an anomaly in the specific heat [3]). This anomaly in the transverse sound velocity is accompanied by either no or, according to new data discussed below, possibly a weak feature in the compressional response measured by a longitudinal sound wave. Second, at the superconducting transition (detected in resistivity and diamagnetic susceptibility [3]), there is a clear discontinuous jump in the shear ultrasound mode. Like other materials, this is accompanied by a jump in the compressional response.

In this work, we performed ultrasound measurements of two new single crystals, which are in the doping range where the quartic state exists according to [3, 4]. The samples had different doping levels $x \sim 0.78$ and 0.8 compared to those measured before. The measurements were performed using a pulse-echo method. The experimental procedure is described in Ref. [3]. The photographs of the samples are shown in Figs. 1a and 2a. The direction of the sound wave propagation was along the longest sample side. The sample thickness used in this study was 10 to 50 μm, which is very thin compared to typically used for ultrasound experiments. This choice is dictated by technical challenges in obtaining thicker homogeneous samples in this doping range. This sample thickness limits the prospect of obtaining optimal ultrasound signals due to possible interference effects. To minimize the effect of the interference, all measurements were performed using short-duration zero echoes (accepting the only first-coming signal). This procedure significantly minimizes the possible interference effects. In this study we restrict ourselves only to qualitative discussion of the character of anomalies but do not perform any quantitative analysis of the jump heights.

For the sample with $x \sim 0.78$, we repeated the measurements of the transverse "B_{1g}" shear mode and longitudinal compressional mode. The results are shown in Fig. 1. The observed behavior of the transverse mode is qualitatively similar to that reported before [3]. In addition, we could not exclude an extra feature at $T_c^{Z_2}$ in the longitudinal sound velocity (Fig. 1b. The possibility for this feature is also consistent with the anomaly in the c_{11} mode at $T_c^{Z_2}$, discussed below. Overall, we have confirmed the results of [3] for the sample with a different doping level, showing that the ultrasound response is qualitatively similar at the quartic and superconducting phase transitions.

The data for the sample $x \sim 0.8$ are summarized in Fig. 2. For this sample we measured the "B_{2g}" shear mode, also know as c_{66}, and the longitudinal compression mode, c_{11}. The data are shown in Fig. 2. There is a pronounced kink at $T_c^{U(1)}$ in c_{66}, and no resolvable response at $T_c^{Z_2}$ in the ultrasound velocity (Fig. 2d). In contrast, c_{11} has a well resolvable anomaly at $T_c^{Z_2}$ and a kink close to $T_c^{U(1)}$ (Fig. 2b). Note that the combination of a non-zero response in the c_{11} mode and a zero response in the c_{66} mode is consistent with a non-zero response in the longitudinal $(c_{11} + c_{22} + 2c_{66})/2$ mode, (Fig. 1b). Our interpretation of the experimental data is shown schematically in Fig. 3.

III. THEORY

A. Formalism

The question we address here is: does the electron quadrupling condensation show itself in the form of singularities in the ultrasound responses? In the quadrupling phase, there is no long-range ordering bilinear in electronic fields (i.e. no order in the superconducting gap/order parameter fields). Furthermore, the mechanism for the formation of the quadrupling state requires fluctuations and is beyond the BCS mean-field approximation [1–4, 6]. Nonetheless, as discussed in models with similar order but in a different context [10, 11], when an appropriate fluctuations-based theory establishes the presence of such phases in a model. Then, the resulting phase diagrams with electron quadrupling can a posteriori be approximately described by using the

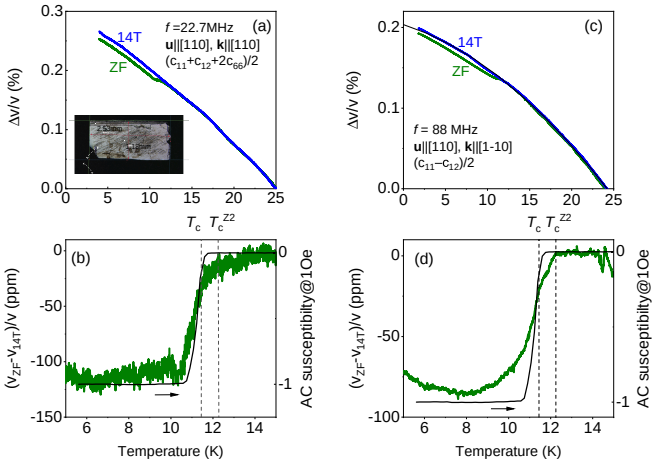

FIG. 1. Temperature dependence of the relative change of the sound velocity (a) for the longitudinal $(c_{11}+c_{12}+2c_{66})/2$ and (c) transverse $(c_{11}-c_{12})/2$ acoustic modes for the $Ba_{1-x}K_xFe_2As_2$ sample with $x = 0.78$. The measurements were done at $f = 22.4$ MHz and $f = 88$ MHz using a transit acoustic signal (zero echo), measured at zero field (ZF) and applied filed 14 T along the sample c-axis. The solid line in panel (c) shows a background fit of the 14 T data. The fitting line was used to plot the data in panel (d). Temperature dependence of the relative change of the sound velocity (b) for the longitudinal $(c_{11}+c_{12}+2c_{66})/2$ and (d) transverse $(c_{11}-c_{12})/2$ acoustic modes (left) with subtracted background measured at 14 T and AC magnetic susceptibility (right) measured at $B \parallel c = 1$O e at $f = 417$ Hz. The data suggest the anomalies for both longitudinal and transverse modes to the quadrupling state.

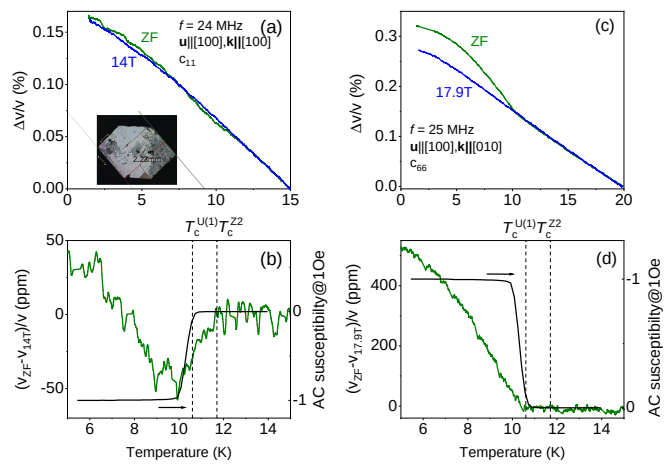

FIG. 2. Temperature dependence of the relative change of the sound velocity (a) for the longitudinal c_{11} and (c) transverse c_{66} acoustic modes for the $Ba_{1-x}K_xFe_2As_2$ sample with $x = 0.8$. The measurements were done at $f = 24$ MHz and $f = 25$ MHz using a transit acoustic signal (zero echo), measured at zero field (ZF) and applied filed along the sample c-axis. Temperature dependence of the relative change of the sound velocity (b) for the longitudinal c_{11} and (d) transverse c_{66} acoustic modes (left) with subtracted background measured in the applied field and inversed AC magnetic susceptibility (right) measured at $B \parallel c = 1$O e at $f = 417$ Hz. The data suggest that the c_{66} mode is not sensitive to the quadrupling state.

"second" mean field approximation. This just means a more general approximant involving (non-independent) order parameters of both superconducting and quadrupling order that phenomenologically describe observed broken symmetries. Following this approach, we will introduce a "quadrupling" order parameter Ψ. In the case of $Ba_{1-x}K_xFe_2As_2$, which breaks time-reversal symmetry, Ψ should share the same symmetry as $\psi_1\psi_2^\dagger$, or, in terms of fermionic creation and annihilation operators, $\Psi \propto < c_1 c_1 c_2^\dagger c_2^\dagger >$. In particular we require that Ψ is gauge invariant and $\Psi + \Psi^\dagger$ is time-reversal symmetric.

We will now develop a minimal model which can reproduce the experimental phase diagram. In order of decreasing temperature, the phase diagram consists of normal, electron quadrupling and broken time-reversal symmetry (BTRS) superconducting phases. The model is constructed from a two-component superconducting order parameter (ψ_1, ψ_2) and the quadrupling order parameter Ψ. The three phases can be described by the field values of the OPs in them: normal ($\psi_i = \Psi = 0$), quadrupling ($\psi_i = 0, \Psi \neq 0$) and BTRS-superconducting ($\psi_1, \psi_2 \neq 0, \mathrm{Im}\ \psi_1\psi_2^\dagger \neq 0$). A schematic plot of our phase diagram is shown in Figure 4.

The free energy must be real and time-reversal-symmetric. A Ginzburg-Landau (GL) model which satisfies all these requirements is

$$\mathcal{F}_V = -\frac{a(T)}{2}\left(|\psi_1|^2 + |\psi_2|^2\right) + \frac{b}{4}\left(|\psi_1|^4 + |\psi_2|^4\right) \quad (1)$$
$$- A_i(T)\Psi_i^2 + A_r\Psi_r^2 + \frac{B_1}{2}\left(\Psi_r^4 + \Psi_i^4\right) + B_2\Psi_r^2\Psi_i^2$$
$$+ c(\psi_1\psi_2^\dagger + \psi_1^\dagger\psi_2)^2 + \frac{\gamma}{4}\left(\Psi\psi_1\psi_2^\dagger + \Psi^\dagger\psi_1^\dagger\psi_2\right) ,$$

where $\Psi = \Psi_r + i\Psi_i$. In the quadrupling phase, the ground state of Ψ will be two-fold degenerate with $\Psi = \pm i|\Psi_0|$. The superconducting and BTRS phase transitions are controlled by the coefficients $a(T)$ and $A_i(T)$. For simplicity, we consider the following temperature dependence of the coefficients:

$$a(T) = \alpha_{SC}(T_c^{\mathrm{U}(1)} - T) \quad (2)$$
$$A_i(T) = \alpha_{\mathrm{BTRS}}(T_c^{\mathrm{Z2}} - T)\,. \quad (3)$$

In these approximations, we aim to reproduce the morphology of the phase diagram of $Ba_{1-x}K_xFe_2As_2$, which is sufficient for our goal of describing the ultrasound response qualitatively. [1]

[1] Note that $Ba_{1-x}K_xFe_2As_2$ has more than two bands, and more general models with a higher number of fields are also considered [3], some comparative discussion between two- and three-component models can be found in [25, 26].

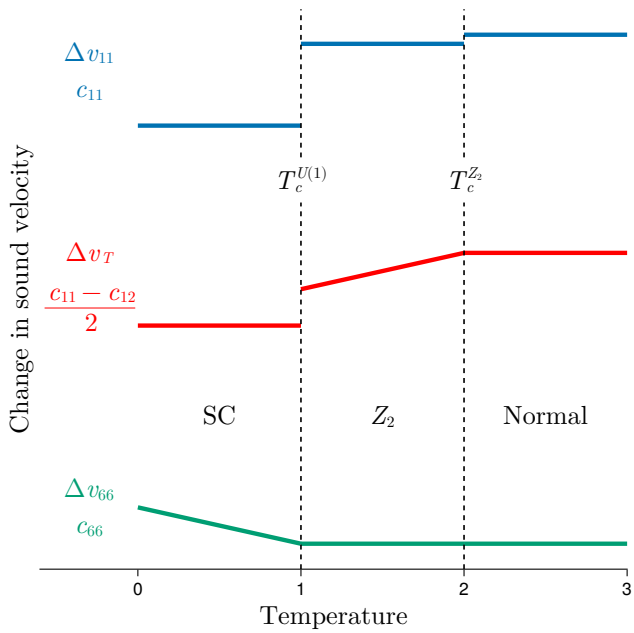

FIG. 3. Our schematic interpretation of all the experimental data: in the Z_2 quadrupling phase, there is a weak signal in the c_{11} mode and a change in gradient in the $c_{11}-c_{12}$ mode. At the superconducting transition, there are jumps in both c_{11} and $c_{11}-c_{12}$ modes but only a change in the gradient in the c_{66} mode.

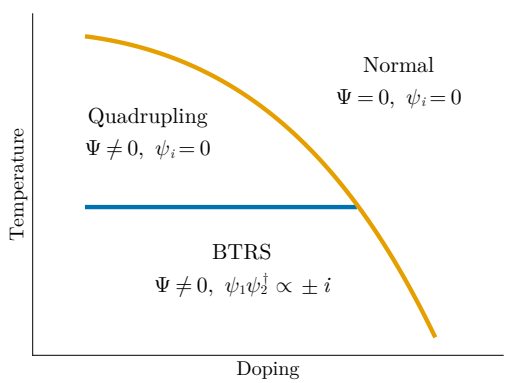

FIG. 4. A schematic plot of our phase diagram with BTRS dome and quartic phase constructed according to experimental data [3, 4, 24]

.

To calculate the ultrasound response we need to couple the order parameters to the strain of the crystal lattice. We do so following [22, 27]. The strain energy is written in terms of the strain tensor $u_{i,j} = 1/2(\partial u_i/\partial x_j + \partial u_j/\partial x_i)$, where u_i is the displacement vector of the underlying crystal lattice. The strain can be labeled by the irreps of the D_{4h} lattice symmetry group of $Ba_{1-x}K_xFe_2As_2$. The combinations $u_{x,x}+u_{y,y}$ and $u_{z,z}$ transform as A_{1g}, $u_{x,x}-u_{y,y}$ transforms as B_{1g}, $u_{x,y}$ transforms as B_{2g} and the pair $(u_{x,z}, u_{y,z})$ transform as E_g. The six independent terms in the elastic energy are given by the six products of these strains that transform as A_{1g}. The elastic constants are usually written in Voigt notation, with two indices. Using this notation, the strain energy is given by

$$\begin{aligned}\mathcal{F}_S =& \frac{c_{11}+c_{12}}{2}\left(u_{x,x}+u_{y,y}\right)^2 + c_{13}(u_{x,x}+u_{y,y})u_{z,z} \\ &+ c_{33}u_{z,z}^2 + \frac{c_{11}-c_{12}}{2}\left(u_{x,x}-u_{y,y}\right)^2 \\ &+ c_{44}\left(u_{x,z}^2+u_{y,z}^2\right) + c_{66}u_{x,y}^2\,. \end{aligned} \tag{4}$$

This is sometimes written in full tensor notation,

$$\mathcal{F}_S = \tfrac{1}{2}c_{ijkl}u_{i,j}u_{k,l}\,. \tag{5}$$

The experimental data is obtained for sound modes which are "in plane". Hence, from now on, we only consider strains in the x-y plane and neglect any strains involving the z-coordinate.

The order parameters (OPs) couple to strain, which ultimately leads to the ultrasound response. The coupling depends on the symmetry of the order parameter. Since we consider the mechanism where the quadrupling OP Ψ has the same symmetry as $\psi_1\psi_2^\dagger$, the symmetry of ψ_1 and ψ_2 uniquely specifies the symmetry of all OPs. We have two goals: first to determine how the quadrupling order parameter couples to ultrasound and second, how this probe can be used to determine the order parameter symmetries. The leading candidates for the superconducting order parameter symmetry of $Ba_{1-x}K_xFe_2As_2$ at magic doping are $s+is$ and $s+id$ states. The analysis of polarization of spontaneous magnetic fields detected in μSR experiments [24] favors the interpretation in terms of the $s+is$ states. However, there is currently not enough certainty about the microscopic details to make a precise model for spontaneous magnetic fields. They are sensitive to detail [28], including the nature of the magnetic-field-inducing disorder and domain wall structure. Hence we'll consider three different OP symmetries: (s,s), $(s,d_{x^2-y^2})$ and vector (d_{xz},d_{yz}). These are representative of the case where the two superconducting order parameters transform as $(A_{1g},A_{1g}),(A_{1g},B_{1g})$ and E_g. Note that the ultrasound signal is similar for nodal and nodeless s-wave models.

The coupling terms that enter the free energy, $\mathcal{F}_C$, are different for the different OP symmetries. We'll consider all terms which are second-order in OP (counting Ψ as quadratic). Then there are four terms that couple to strain. They are

$$|\psi_1|^2+|\psi_2|^2,\ |\psi_1|^2-|\psi_2|^2,\ \psi_1\psi_2^\dagger+\psi_1^\dagger\psi_2\,,\ \Psi+\Psi^\dagger. \tag{6}$$

We will also include coupling to the higher-order term

$$|\Psi|^2\,, \tag{7}$$

which will be important to describe the weak signal in the quadrupling phase of the longitudinal mode. These

terms couple to different strains depending on the OP symmetry.

(s,s) OP symmetry: all terms couple to the A_{1g} strain. The free energy term which couples strain and the OPs is given by

$$\mathcal{F}_C^{s,s} = \big(\delta_1(|\psi_1|^2+|\psi_2|^2)+\delta_2(|\psi_1|^2-|\psi_2|^2)+ \tag{8}$$
$$\delta_3(\psi_1\psi_2^\dagger+\psi_1^\dagger\psi_2)+\tfrac{\delta_4}{2}(\Psi+\Psi^\dagger)+\delta_5|\Psi|^2\big)(u_{x,x}+u_{y,y})\,.$$

$(s,d_{x^2-y^2})$ OP symmetry: the mixed bilinears transform as B_{1g}. Hence they couple to $u_{xx}-u_{yy}$, giving the coupling free energy

$$\begin{aligned}\mathcal{F}_C^{s,d} &= \big(\delta_1(|\psi_1|^2+|\psi_2|^2)+\delta_2(|\psi_1|^2-|\psi_2|^2)\\ &+\delta_5|\Psi|^2\big)(u_{x,x}+u_{y,y})\\ &+\big(\delta_3(\psi_1\psi_2^\dagger+\psi_1^\dagger\psi_2)+\tfrac{\delta_4}{2}(\Psi+\Psi^\dagger)\big)(u_{x,x}-u_{y,y})\end{aligned} \tag{9}$$

(d_{xz},d_{yz}) OP symmetry: the simplest vector OP that transforms like the E_g irrep. It couples to strain as follows

$$\begin{aligned}\mathcal{F}_C^{d,d} =&(\delta_1(|\psi_1|^2+|\psi_2|^2)+\delta_5|\Psi|^2)(u_{x,x}+u_{y,y})\\ &+\delta_2(|\psi_1|^2-|\psi_2|^2)(u_{x,x}-u_{y,y})\\ &+\big(\delta_3(\psi_1\psi_2^\dagger+\psi_1^\dagger\psi_2)+\tfrac{\delta_4}{2}(\Psi+\Psi^\dagger)\big)u_{x,y}\,.\end{aligned} \tag{10}$$

In all three cases, the strain-OP coupling free energy can be written as

$$\mathcal{F}_C = \Gamma_{ij}(\psi,\Psi)u_{i,j}\,. \tag{11}$$

We have now found the free energy for our theory, including strain coupling. We now develop the theory of ultrasound response for a class of theories, including ours. Consider a model with order parameters Π_a, symmetric strain tensor $u_{i,j}$ and linear strain coupling. The total free energy can be written as

$$\mathcal{F} = V(\Pi)+\tfrac{1}{2}c_{ijkl}u_{i,j}u_{k,l}+\Gamma_{ij}(\Pi)u_{i,j}\,. \tag{12}$$

This has solution (Π^0,u^0), which satisfies the static equations of motion

$$\frac{\partial}{\partial\Pi_a}\left(V-\tfrac{1}{2}\Gamma_{ij}c^{-1}_{ijkl}\Gamma_{kl}\right)\bigg|_{\Pi=\Pi^0}=0 \tag{13}$$
$$u^0_{i,j}=c^{-1}_{ijkl}\Gamma_{kl}(\Pi^0) \tag{14}$$

Naively, the four-tensor c_{ijkl} does not have a unique inverse. However, since it is symmetric in $i\leftrightarrow j$ and $k\leftrightarrow l$, it does have a unique inverse with the same symmetry.

We are interested in perturbations around the ground state solution $\Pi^0, u^0_{i,j}$. Denote these are $\Pi_a=\Pi^0_a+\eta_a$ and $u=u^0+u^{\rm wv}$. One must be careful here, and quotient out gauge transformations. We can do this by choosing the perturbations to be physical, gauge invariant η. We won't be explicit as the details depend on whether it is in the superconducting or quartic phase.

$$\mathcal{F}_2=\tfrac{1}{2}\left(V_{ab}+\Gamma_{ij,ab}\partial_j u^0_i\right)\eta_a\eta_b \tag{15}$$
$$+\tfrac{1}{2}c_{ijkl}u^{\rm wv}_{i,j}u^{\rm wv}_{k,l}+\eta_a\Gamma_{ij,a}u^{\rm wv}_{i,j}\,. \tag{16}$$

where $,a=\frac{\partial}{\partial\Pi_a}|_{\Pi^0}$. The equations of motion for the perturbations are

$$\tau_0\frac{\partial\eta_a}{\partial t}+(V_{ab}+\Gamma_{ij,ab}\partial_j u^0_i)\eta_b+\Gamma_{ij,a}u^{\rm wv}_{i,j}=0 \tag{17}$$
$$\rho\ddot{u}^{\rm wv}_i-\partial_j\left(c_{ijkl}u^{\rm wv}_{k,l}+\eta_a\Gamma_{ij,a}\right)=0\,, \tag{18}$$

which have solutions

$$\eta_a=A_a e^{ik_ix_i-i\omega t},\quad u^{\rm wv}_i=U_ie^{ik_ix_i-i\omega t}\,. \tag{19}$$

The ansatz gives the dispersion relation

$$\rho\omega^2U_i-c_{ijkl}k_jk_lU_k+\Gamma_{ij,a}\tilde{V}^{-1}_{ab}\Gamma_{kl,b}k_jk_lU_k=0\,, \tag{20}$$

where

$$\tilde{V}_{ab}=\left(V_{ab}+\Gamma_{ij,ab}\partial_j u^0_i-i\omega\tau_0\delta_{ab}\right)\,. \tag{21}$$

Different sound modes then correspond to different choices of $\boldsymbol{k}$ and $\boldsymbol{U}$ in the dispersion relation. We are particularly interested in three modes, the longitudinal, transverse and the B_{2g} mode. The longitudal wave corresponds to the choice $\boldsymbol{U}=(1,0,0)$ and $\boldsymbol{k}=(k_{11},0,0)$, the transverse wave to $\boldsymbol{U}=(1,1,0)/\sqrt{2}$ and $\boldsymbol{k}=(k_T,-k_T,0)/\sqrt{2}$, and the B_{2g} mode to $\boldsymbol{U}=(1,0,0)$ and $\boldsymbol{k}=(0,k_{66},0)/\sqrt{2}$. Substituting these into the dispersion relation, we can find $k_{11/T/66}(\omega)$ and then the sound velocity is given by

$$v_{11/T/66}=\frac{\omega}{\text{Re }k_{11/T/66}(\omega)}\,. \tag{22}$$

For analytic results, we take the large c, small τ_0 limit. In this limit the rescaled and renormalised change in sound velocity, relative to the normal state sound velocity v^0, is

$$\Delta\tilde{v}=c^0\frac{v-v^0}{v^0}=-\frac{1}{2}\Gamma_{ij,a}\tilde{V}^{-1}_{ab}\Gamma_{kl,b}U_i\hat{k}_jU_k\hat{k}_l\,, \tag{23}$$

where c^0 is the probed elastic coefficient for each mode. For the longitudinal mode, $c^0_{11}=c_{11}$, for the transverse mode $c^0_T=(c_{11}-c_{12})/2$ and for the B_{2g} mode $c^0_{66}=c_{66}$. The normal sound velocity is closely related, given by $v^0_{11/T/66}=\sqrt{\rho/c^0_{11/T/66}}$.

B. Results

1. $\gamma=0$ case. Analytically tractable toy model

In the beginning, we investigate a toy model without coupling between superconducting and quadrupling order parameters. The advantage of this model is that we can investigate it analytically and inspect the roles played by some of the terms. Here the free energy is given by (1) with $\gamma=0$ and

$$a(T)=\alpha_{SC}(T_{\rm c}^{\rm U(1)}-T) \tag{24}$$
$$A_i(T)=\alpha_{\rm BTRS}(T_{\rm c}^{\rm Z2}-T)\,, \tag{25}$$

and $T_c^{U(1)} < T_c^{Z2}$. We consider the case where there is no bilinear Josephson term.

The quadrupling phase occurs when $A_i > 0$ but $a < 0$. The superconducting order parameters are zero in this phase and, if $A_r > 0$, the only non-zero order parameter is Ψ_i, equal to

$$\Psi_i^2 = \frac{A_i}{B_1}\,. \tag{26}$$

The ultrasound response at the quadrupling phase transition for the (s,s) model is

$$\Delta\tilde{v}_{11} = \delta_4^2 D_4 - \frac{\delta_5^2}{2B_1}\,, \quad \Delta\tilde{v}_T = \Delta\tilde{v}_{66} = 0 \tag{27}$$

where

$$D_4 = \frac{A_i B_2}{4A_iA_rB_2 + 4A_r^2B_1}\,. \tag{28}$$

The only non-zero response is in the c_{11} mode. In contrast, the $(s, d_{x^2-y^2})$ model has the result

$$\Delta\tilde{v}_{11} = -\frac{\delta_5^2}{2B_1}, \quad \Delta\tilde{v}_T = \delta_4^2 D_4, \quad \Delta\tilde{v}_{66} = 0\,. \tag{29}$$

The non-zero response in the transverse mode is linear in T for small A_i (equivalently, near the transition), as seen by a Taylor expansion:

$$D_4 \sim -\frac{\alpha_{\rm BTRS} B_2 (T - T_{\rm BTRS})}{4A_r^2 B_1}\,. \tag{30}$$

Hence there is a negative, linear slope provided $B_2 < 0$. Finally the (d_{xz}, d_{yz}) OP has the response

$$\Delta\tilde{v}_{11} = -\frac{\delta_5^2}{2B_1}, \quad \Delta\tilde{v}_T = 0, \quad \Delta\tilde{v}_{66} = \delta_4^2 D_4\,. \tag{31}$$

Overall, a non-zero response in the transverse mode is only present for the $(s, d_{x^2-y^2})$ model.

At the superconducting transition, the superconducting order parameters turn on. We assume that $c > 0$ so that the superconducting order parameters have broken time-reversal symmetry. Since they are not coupled to the quadrupling phase, we can find analytic expressions for the solutions:

$$\psi_1^2 = -\psi_2^2 = \frac{a}{b-2c}\,. \tag{32}$$

Note that in the superconducting phase of the decoupled model there are four degenerate ground states, meaning that the symmetry is broken to a group with an extra Z_2 symmetry: $U(1) \times Z_2 \times Z_2$. This deficiency of the toy model will be fixed when we include a non-zero coupling γ.

Having found the ground state solutions, we substitute them into equation (23) to find the ultrasound response, which depends on the chosen order parameter symmetry. In the three cases we consider, the response is

$$\begin{aligned}
(s,s):\ \Delta\tilde{v}_{11} &= \delta_4^2 D_4 - \frac{2\delta_1^2}{b-2c} - \frac{2\delta_2^2}{b+2c} - \frac{\delta_3^2}{8c} - \frac{\delta_5^2}{2B_1}\\
\Delta\tilde{v}_T &= \Delta\tilde{v}_{66} = 0.\\
(s,d):\ \Delta\tilde{v}_{11} &= -\frac{2\delta_1^2}{b-2c} - \frac{2\delta_2^2}{b+2c} - \frac{\delta_5^2}{2B_1}\\
\Delta v_T &= \delta_4^2 D_4 - \frac{\delta_3^2}{8c}\\
\Delta\tilde{v}_{66} &= 0.\\
(d,d):\ \Delta\tilde{v}_{11} &= -\frac{2\delta_1^2}{b-2c} - \frac{\delta_5^2}{2B_1}\\
\Delta\tilde{v}_T &= -\frac{2\delta_2^2}{b+2c}\\
\Delta\tilde{v}_{66} &= \delta_4^2 D_1 - \frac{\delta_3^2}{8c}
\end{aligned}$$

The results are nontrivial. The most important fact is that there are jumps in the transverse sound mode in both the (s,d) and (d,d) models but not in the (s,s) model. Hence, the jump at the superconducting transition in the transverse mode, which is clearly seen in the experimental data, cannot be described by this toy (s,s) model.

2. $\gamma \neq 0$ case

We now present results for a more realistic model which includes coupling between Ψ and the ψ. The free energy for the order parameters is given in equation (1) with

$$(b, A_r, c, B_1, B_2, \gamma) = (1, 0.4, 0.2, 1, -0.1, -0.2)\,. \tag{33}$$

Due to the non-zero γ term, there are no explicit formulae for the order parameters in each phase, though we can find them as a series in γ. The results to first order are

$$\text{Quadrupling: } \Psi^2 = -A_i/B_1, \psi = 0 \tag{34}$$

$$\text{SC: } \Psi = i\left(\sqrt{A_i/B_1} + \gamma\frac{a}{8A_i(b-2c)}\right),$$

$$\psi_1\psi_2^\dagger = i\left(\frac{a}{b-2c} - \gamma\frac{\sqrt{A_i}}{2\sqrt{B_1}(b-2c)}\right).$$

The coupling between strain and the OPs depends on the OP symmetry and are given by (8)-(10) with $\delta_i = 1, i = 1-4$ and $\delta_5 = 0.7$ (since δ_5 is the coefficient of a higher order term) and the phase transition temperatures are controlled by

$$A_i = T_c^{Z2} - T = 2 - T \tag{35}$$

$$a = T_c^{U(1)} - T = 1 - T\,. \tag{36}$$

The results for the (s,s), $(s, d_{x^2-y^2})$ and (d_{xz}, d_{yz}) models are shown in Figure 5. The coupling between superconducting and quadrupling order parameters smooths out the ultrasound responses but still produces a jump of the scale seen in the experimental data.

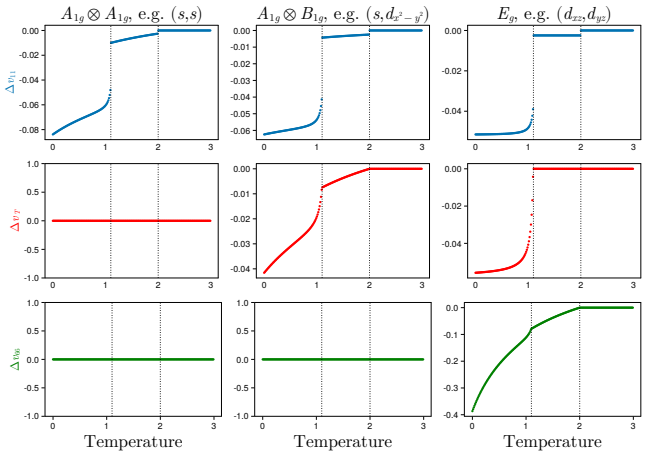

FIG. 5. The ultrasound response in the longitudinal, transverse B_{1g} (or $(c_{11}-c_{12})/2$) and B_{2g} (or c_{66}) modes, in the models defined in (1). The $s, d_{x^2-y^2}$ model reproduces: a linear change with temperature in the transverse mode at the quadrupling transition $T = T_c^{Z_2} = 2$, no response in the longitudinal mode at the quadrupling transition and jumps in both at the superconducting transition $T = T_c^{U(1)} = 1$.

The (s,s) model has a linear response in the quadrupling state and a jump at the superconducting transition for the longitudinal mode. There is no response for the transverse $(c_{11}-c_{12})/2)$ mode. The (s,d) model has a linear response in this transverse mode and a small signal in the longitudinal c_{11} mode[2] in the quadrupling phase, and a jump in both modes at the superconducting transition. The (d,d) model has a linear response in the longitudinal mode in the quadrupling phase and a jump in both transverse modes at the superconducting transition.

The experimental data suggests that there is a weak signal in the longitudinal mode ((c_{11}) and a linear response in the transverse mode ($(c_{11}-c_{12})/2$) in the quadrupling phase, and a jump in both these modes at the superconducting transition. This best matches the $(s, d_{x^2-y^2})$ model. Hence, based on ultrasound data alone, the most likely order parameter symmetry is $(s, d_{x^2-y^2})$.

The vector OP (d_{xz}, d_{yz}) produces jumps at the superconducting and quadrupling transitions but has no ultrasound response in the transverse mode in the quadrupling phase. As we will see in Section IV C, higher-order terms can produce a weak signal in the quadrupling phase. Hence the data can also in principle be described using an OP with this vector symmetry.

[2] This implies there is also a small signal in the $(c_{11}+c_{12}+2c_{66})/2$ mode. This mode was measured in a previous experiment [3], which shows no strong signal in this mode.

IV. s-WAVE MODELS

Momentum space symmetry of the order parameters in $Ba_{1-x}K_xFe_2As_2$ remains a subject of discussion. Initially, several experiments were interpreted in favor of a d-wave order parameter in KFe_2As_2 ($x = 1$) including thermal conductivity, and specific heat [29, 30]. However, as mentioned above, the μSR data favors the scenario that the order parameter is s-wave [24] at doping $x \approx 0.8$. Recent ARPES data at $x = 1$ is also consistent with an $s_\pm$ order parameter [31]. Near optimal doping ($x \approx 0.4$), ARPES [32, 33] and thermal conductivity [34] data suggest that the order parameter is s-wave and isotropic. Below optimal doping, the gap becomes anisotropic and develops extrema [35], though it is still typically thought to be s-wave. However, our considerations suggest that there is no ultrasound response in the transverse sound modes for the simplest $s + is$ order parameter. This is inconsistent with the experimental data that suggests there should be a linear response, then a jump. Hence, we now explore possible modifications to the s-wave theory, which might produce the desired nontrivial response. In this subsection, we always assume that the superconducting OP transforms as (s,s) and the quadrupling OP is s-wave.

A. Nematicity

First, let us consider the possibility of nematicity so that the lattice symmetry changes in the quadrupling state. The original lattice has D_{4h} symmetry. The experimental data suggest there is some enhanced nematic susceptibility consistent with the proximity of "[110]" nematic critical point close to $x = 0.8$. This stretches the square-like original lattice into a diamond, breaking the D_{4h} symmetry to C_{2h} [36]. Hence 90° rotations (which form a C_4 subgroup) are broken to 180° rotations.

Consider now the case that such nematicity of some origin was present in the quadrupling state. The symmetry breaking means we have to reanalyze the group and representation theory. Most significantly, the strain $u_{x,y}$ now transforms as A_{1g}. Hence it can couple to the quadratic OP terms (41). The uniaxial strain $u_{x,x} - u_{y,y}$ still transforms as B_{1g} and so can't couple to the s-wave OPs. The new free energy term describing the coupling between strain and the OPs is

$$\begin{aligned}\mathcal{F}_C^{s,s} = \big(&\gamma_1(|\psi_1|^2 + |\psi_2|^2) + \gamma_2(|\psi_1|^2 - |\psi_2|^2) \\ &+ \gamma_3(\psi_1\bar{\psi}_2 + \bar{\psi}_1\psi_2) + \gamma_4(\Psi + \Psi^\dagger)\big)(u_{x,x} + u_{y,y})\,. \\ &\big(\gamma_5(|\psi_1|^2 + |\psi_2|^2) + \gamma_6(|\psi_1|^2 - |\psi_2|^2) \\ &+ \gamma_7(\psi_1\bar{\psi}_2 + \bar{\psi}_1\psi_2) + \gamma_8(\Psi + \Psi^\dagger)\big)u_{x,y}\,.\end{aligned} \tag{37}$$

We expect that $\gamma_{5,6,7,8}$ are small, proportional to the size of the symmetry breaking. We can model these terms simply by modifying Γ_{ij} in the formalism of Section III A. We find that the new terms, with coefficients $\gamma_{5,6,7,8}$, create a non-zero response in the longitudinal sound mode

and no additional response in the traverse B_{1g} mode. Hence the experimentally observed character of nematic susceptibility [36] cannot explain the ultrasound response in this transverse mode.

We have considered the possibility of a nematic order in the quadrupling state, breaking a certain symmetry. This does produce an ultrasound response, but not in the desired transverse mode. Theoretically, a response in this mode requires "XY" nematicity, which is ruled out in [36].

B. External stress

Suppose that the system was externally stressed uniaxially, by the constant force $\sigma^0_{xx} - \sigma^0_{yy}$. This force transforms as B_{1g} and its product with $u_{xx} - u_{yy}$ is invariant under all symmetry transformations. Hence the product couples to any gauge invariant functions of the order parameter. In detail, the terms

$$\left(\sigma^0_{xx} - \sigma^0_{yy}\right)\left(u_{x,x} - u_{y,y}\right)\Big(\alpha_1(|\psi_1|^2 + |\psi_2|^2) + \alpha_2(|\psi_1|^2 - |\psi_2|^2) + \alpha_3\left(\psi_1\psi_2^\dagger + \psi_1^\dagger\psi_2\right) + \alpha_4(\Psi + \Psi^\dagger)\Big) \tag{38}$$

should be added to the free energy. This can be modeled using the framework developed in Section III A by updating the tensor Γ_{ij}.

In the decoupled limit, the newly added term gives an ultrasound response

$$\Delta\tilde{v}_T = \left(\sigma^0_{xx} - \sigma^0_{yy}\right)^2\left(\alpha_4^2 D_4 - \frac{2\alpha_1^2}{b-2c} - \frac{2\alpha_2^2}{b+2c} - \frac{\alpha_3^2}{8c}\right), \tag{39}$$

corresponding to a linear response in the quadrupling phase and a jump at the superconducting transition, matching experimental data.

The presence of external stress on the system can explain the experimental data. However, for this to be a reasonable explanation, we must argue why an external stress of the type $\sigma^0_{xx} - \sigma^0_{yy}$ might be present. Stresses of the type σ^0_{xy} and $\sigma^0_{xx} + \sigma^0_{yy}$ would lead to signals in the longitudinal data. Note that the ultrasound response in the longitudinal modes are weak.

C. Higher order strain coupling

All combinations of an (s, s) order parameter transform as A_{1g}. These can couple to higher order products of the strain tensor. The simplest are terms quadratic in strain. The possible terms, which affect strain in the plane, are

$$(u_{xx} + u_{yy})^2, (u_{xx} - u_{yy})^2, u_{xy}^2 \tag{40}$$

All three of these can couple to any quadratic terms of the OP

$$|\psi_1|^2 + |\psi_2|^2, |\psi_1|^2 - |\psi_2|^2, \psi_1^\dagger\psi_2 + \psi_1\psi_2^\dagger, \Psi + \Psi^\dagger\,. \tag{41}$$

We'll also consider terms of the form $|\Psi|^2$. So overall, there are fifteen terms of this kind. We can write the free energy contribution of these terms in tensor notation:

$$F_{ijkl}(\psi, \Psi)u_{ij}u_{kl} \tag{42}$$

If we assume that the c_{ijkl} defined in (4) are large, and hence u_0 is small, the formalism from earlier is only slightly modified. The dispersion relation (20) is only modified by

$$c_{ijkl} \to (c + F(\psi_0, \Psi_0))_{ijkl}\,. \tag{43}$$

and so the sound velocity for the transverse sound wave in the normal state is simply

$$v_T^0 = \sqrt{c_{11} - c_{12} + F_{1111} - F_{1122}}\,. \tag{44}$$

And the normalised change in v_T, in a large c expansion, is given by

$$\frac{v_T - v_T^0}{v_T^0} \approx \frac{F_{1111} - F_{1122}}{2(c_{11} - c_{12})} \tag{45}$$

This expression can be written in terms of the order parameters, as follows

$$F_{1111} - F_{1122} = f_1\left(|\psi_1|^2 + |\psi_2|^2\right) + f_2\left(|\psi_1|^2 - |\psi_2|^2\right) f_3\left(\psi_1^\dagger\psi_2 + \psi_1\psi_2^\dagger\right) + f_4\left(\Psi + \Psi^\dagger\right) + f_5|\Psi|^2\,, \tag{46}$$

with some new parameters f_i. So far in this paper we have modeled the phase transitions as being second order. Hence the square of each order parameter grows approximately linearly with T near T_c. As a result, the terms in Eq. 46 are continuous across the phase transition: the new couplings generate a change in the slope of the ultrasound response. Hence, these terms cannot account for the discontinuous jump in the ultrasound data across the superconducting transition when the phase transition is second order. However, it can account for the change in slope in the c_{66} data from Figure 2e.

D. First order phase transition

In general, the phase transition from quartic to superconducting state can be first order when quartic phase is not too large. This is seen in Monte-Carlo simulations of similar models where, near the bicritical point, the phase transitions can be first order [2]. It was first pointed out and studied in detail in related models with different symmetry[37, 38]. Our simple model (1) also contains a first-order phase transition from the quadrupling to BTRS superconducting phase when A_i, and hence Ψ, are small. We can model this using the parameters

$$(a(T), A_i, b, A_r, c, B_1, B_2, \gamma) = (1 - T, \min(0.02, 2 - T), 1, 0.4, 0.2, 1, -0.1, -0.2)\,. \tag{47}$$

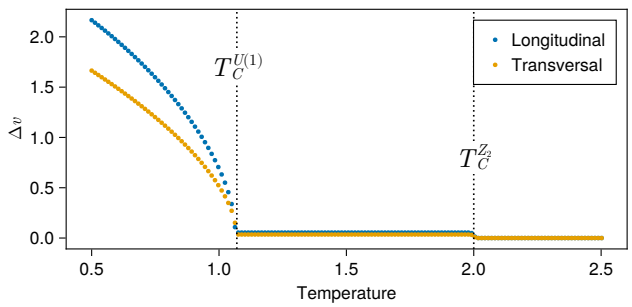

FIG. 6. A typical ultrasound response when there is a first-order phase transition and higher order strain coupling, for an s-wave model. There is a small non-zero response in the quadrupling phase and a jump at $T_c^{U(1)}$ in all sound modes.

One can check that the order parameters change discontinuously over $T = 1$. We then also include the higher-order strain terms

$$\left(|\psi_1|^2 + |\psi_2|^2\right)\left(f_1(u_{11} - u_{22})^2 + g_1(u_{11} + u_{22})^2\right) + |\Psi|^2\left(f_5(u_{11} - u_{22})^2 + g_5(u_{11} + u_{22})^2\right) . \quad (48)$$

The ultrasound response is seen in Figure 6. We see that there are weak responses in the quadrupling phase (due to non-zero g_5 and f_5) and a discontinuity in the data at the superconducting transition. The discontinuities are due to the fact the phase transition is first order. This relies on the fact that A_i is small here. However, A_i also controls the size of Ψ_i^2 and this controls the size of the response in the quadrupling phase. So it seems difficult to construct a model of this kind with a large response in the quadrupling phase and a large jump at $T_c^{U(1)}$. Also note that the transitions in these models are very weakly first order [2, 38]. These models do not contradict the experimental observations since the existing calorimetry data cannot resolve the order of the phase transition [3, 4].

E. Derivative coupling

In the BTRS phase of $Ba_{1-x}K_xFe_2As_2$, there are spontaneous magnetic fields whose value increases with decreasing temperature. These have been observed in the superconducting state at magic doping [24] and in the quadrupling state [3]. For a recent theoretical work on the origin of these fields, see [25]. The spontaneous magnetic fields imply persistent currents and hence existence of stationary nonzero gradient terms. Nonzero gradient terms are important to describe muon spin rotation data of $Ba_{1-x}K_xFe_2As_2$ and hence, their potential role in the ultrasound response should be assessed. The allowed gradient terms depend on the order parameter symmetry, with a variety of consequences [28, 39].

There are OP derivative terms which couple to the strain. One derivative term which couples to the B_{1g} strain to an s-wave OP is

$$\left(|\mathcal{D}_x\Psi|^2 - |\mathcal{D}_y\Psi|^2\right)(u_{xx} - u_{yy}) . \quad (49)$$

Such terms will only produce an ultrasound response where the order parameter is inhomogeneous: near defects, domain walls and surfaces. The term (49) is only nonzero for non-axially symmetric defects in the simplest $s + is$ models. Microscale non-axially-symmetric defects lead to the appearance of spontaneous magnetic fields on relatively large scales in the simplest $s + is$ models [40]. Understanding this response, and whether it can be large enough to be seen in ultrasound experiments, will require an elaboration on defects structure in the material and significant additional modeling.

V. CONCLUSIONS

In conclusion, we obtained new experimental data and developed a theory of ultrasound response in the electron quadrupling phase.

Our main result is that the ultrasound is sensitive to the phase transition in the electron quadrupling state. The theoretical models with time-reversal-symmetry breaking electron quadrupling state are shown to be consistent with those observed in ultrasound experiments on $Ba_{1-x}K_xFe_2As_2$. This explains why such singularities correlate with singularities in the specific heat observed at the time-reversal symmetry breaking and superconducting transition temperatures [3, 4].

We have also discussed how the ultrasound response depends on the symmetry of the electron quadrupling order parameters, which will pave the way to ascertain the symmetry of the quadrupling phases in future works. In a simple GL model, the experimental data coincides with our model of quadrupling order arising from a low-temperature $s + id_{x^2-y^2}$ superconducting state. By contrast, the analysis of polarization of spontaneous magnetic fields in the superconducting state [24] was more naturally explained by the model where the low-temperature phase is an $s+is$-superconductor. Nonetheless, we stress that experimental data is inconsistent only with the simplest $s+is$-models and we discussed multiple generalizations of $s + is$-models with additional inputs, such as explicit rotation-symmetry breaking by strain or defects in an $s + is$ state can produce such a response. The precise detail of the order parameter remains an interesting question requiring a combination of further experimental and theoretical investigations.

Hence our overall conclusion is that ultrasound data is consistent with the existence of two transitions in $Ba_{1-x}K_xFe_2As_2$: the upper transition at $T_c^{Z_2}$ corresponding to an electron quadrupling state breaking time-reversal symmetry and the lower one at $T_c^{U(1)}$ corresponding to the onset of superconductivity.

VI. ACKNOWLEDGEMENTS

CH is supported by the Carl Trygger Foundation through the grant CTS 20:25. EB was supported by the Swedish Research Council Grants 2022-04763, by Olle Engkvists Stiftelse, and partially by the Wallenberg Initiative Materials Science for Sustainability (WISE) funded by the Knut and Alice Wallenberg Foundation. VG is supported by the NSFC grants 12374139 and 12350610235. We acknowledge support of the HLD at HZDR, member of the European Magnetic Field Laboratory (EMFL).

[1] T. A. Bojesen, E. Babaev, and A. Sudbø, Time reversal symmetry breakdown in normal and superconducting states in frustrated three-band systems, Phys. Rev. B **88**, 220511 (2013).

[2] T. A. Bojesen, E. Babaev, and A. Sudbø, Phase transitions and anomalous normal state in superconductors with broken time-reversal symmetry, Phys. Rev. B **89**, 104509 (2014).

[3] V. Grinenko, D. Weston, F. Caglieris, C. Wuttke, C. Hess, T. Gottschall, I. Maccari, D. Gorbunov, S. Zherlitsyn, J. Wosnitza, A. Rydh, K. Kihou, C.-H. Lee, R. Sarkar, S. Dengre, J. Garaud, A. Charnukha, R. Hühne, K. Nielsch, B. Büchner, H.-H. Klauss, and E. Babaev, State with spontaneously broken time-reversal symmetry above the superconducting phase transition, Nat. Phys. , 1254–1259 (2021).

[4] I. Shipulin, N. Stegani, I. Maccari, K. Kihou, C.-H. Lee, Y. Li, R. Hühne, H.-H. Klauss, M. Putti, F. Caglieris, et al., Calorimetric evidence for two phase transitions in $ba_{1-x}k_xfe_2as_2$ with fermion pairing and quadrupling states, Nature Communications **14**, 6734 (2023).

[5] Y.-G. Zheng, A. Luo, Y.-C. Shen, M.-G. He, Z.-H. Zhu, Y. Liu, W.-Y. Zhang, H. Sun, Y. Deng, Z.-S. Yuan, and J.-W. Pan, Observation of counterflow superfluidity in a two-component mott insulator (2024), arXiv:2403.03479 [cond-mat.quant-gas].

[6] E. Babaev, A. Sudbø, and N. Ashcroft, A superconductor to superfluid phase transition in liquid metallic hydrogen, Nature **431**, 666 (2004).

[7] E. Babaev, Phase diagram of planar $u(1) \times u(1)$ superconductor: Condensation of vortices with fractional flux and a superfluid state, Nucl. Phys. B **686**, 397 (2004).

[8] J. Smiseth, E. Smørgrav, E. Babaev, and A. Sudbø, Field- and temperature-induced topological phase transitions in the three-dimensional n-component london superconductor, Phys. Rev. B **71**, 214509 (2005).

[9] A. B. Kuklov, M. Matsumoto, N. V. Prokof'ev, B. V. Svistunov, and M. Troyer, Deconfined criticality: Generic first-order transition in the su(2) symmetry case, Phys. Rev. Lett. **101**, 050405 (2008).

[10] A. Kuklov, N. Prokof'ev, B. Svistunov, and M. Troyer, Deconfined criticality, runaway flow in the two-component scalar electrodynamics and weak first-order superfluid-solid transitions, Ann. Phys. **321**, 1602 (2006), july 2006 Special Issue.

[11] B. Svistunov, E. Babaev, and N. Prokofev, Superfluid States of Matter (CRC Press, 2015).

[12] D. Agterberg and H. Tsunetsugu, Dislocations and vortices in pair-density-wave superconductors, Nature Physics **4**, 639 (2008).

[13] E. Berg, E. Fradkin, and S. A. Kivelson, Charge-4e superconductivity from pair-density-wave order in certain high-temperature superconductors, Nature Physics **5**, 830 (2009).

[14] L. Radzihovsky and A. Vishwanath, Quantum liquid crystals in an imbalanced fermi gas: Fluctuations and fractional vortices in larkin-ovchinnikov states, Phys. Rev. Lett. **103**, 010404 (2009).

[15] Y. Iguchi, R. Shi, K. Kihou, C. Lee, M. Barkman, A. Benfenat, V. Grinenko, E. Babaev, and K. Moler, Superconducting vortices carrying a temperature-dependent fraction of the flux quantum, Science **380**, 1244 (2023).

[16] L. Hebel and C. Slichter, Nuclear relaxation in superconducting aluminum, Physical Review **107**, 901 (1957).

[17] B. Golding, D. Bishop, B. Batlogg, W. Haemmerle, Z. Fisk, J. Smith, and H. Ott, Observation of a collective mode in superconducting u be 13, Physical review letters **55**, 2479 (1985).

[18] V. Müller, D. Maurer, E.-W. Scheidt, C. Roth, K. Lüders, E. Bucher, and H. Bömmel, Observation of a lambda-shaped ultrasonic attenuation peak in superconducting upt3, Solid state communications **57**, 319 (1986).

[19] M. Tinkham, Introduction to superconductivity (Courier Corporation, 2004).

[20] S. Ghosh, M. Matty, R. Baumbach, E. D. Bauer, A. Shekhter, J. Mydosh, E.-A. Kim, and B. Ramshaw, One-component order parameter in uru2si2 uncovered by resonant ultrasound spectroscopy and machine learning, Science advances **6**, eaaz4074 (2020).

[21] S. Benhabib, C. Lupien, I. Paul, L. Berges, M. Dion, M. Nardone, A. Zitouni, Z. Q. Mao, Y. Maeno, A. Georges, L. Taillefer, and C. Proust, Ultrasound evidence for a two-component superconducting order parameter in sr_2ruo_4, Nature Physics **17**, 194–198 (2021).

[22] M. Sigrist, Ehrenfest relations for ultrasound absorption in sr_2ruo_4, Progress of Theoretical Physics **107**, 917 (2002).

[23] S. Ghosh, A. Shekhter, F. Jerzembeck, N. Kikugawa, D. A. Sokolov, M. Brando, A. Mackenzie, C. W. Hicks, and B. Ramshaw, Thermodynamic evidence for a two-component superconducting order parameter in sr2ruo4, Nature Physics **17**, 199 (2021).

[24] V. Grinenko, R. Sarkar, K. Kihou, C. H. Lee, I. Morozov, S. Aswartham, B. Büchner, P. Chekhonin, W. Skrotzki, K. Nenkov, R. Hühne, K. Nielsch, S. L. Drechsler, V. L. Vadimov, M. A. Silaev, P. Volkov, I. Eremin, H. Luetkens, and H. H. Klauss, Superconductivity with broken time-reversal symmetry inside a superconducting s-wave state, Nat. Phys. **16**, 789–794 (2020).

[25] J. Garaud and E. Babaev, Effective model and magnetic properties of the resistive electron quadrupling state, Phys. Rev. Lett. , 087602 (2022).

[26] J. Garaud, M. Silaev, and E. Babaev, Microscopically derived multi-component ginzburg–landau theories for s+is

superconducting state, Physica C **533**, 63 (2017), ninth international conference on Vortex Matter in nanostructured Superdonductors.

[27] B. Lüthi, Physical acoustics in the solid state, Vol. 148 (Springer Science & Business Media, 2007).

[28] A. Benfenati, M. Barkman, T. Winyard, A. Wormald, M. Speight, and E. Babaev, Magnetic signatures of domain walls in s+ i s and s+ i d superconductors: Observability and what that can tell us about the superconducting order parameter, Physical Review B **101**, 054507 (2020).

[29] J.-P. Reid, M. A. Tanatar, A. Juneau-Fecteau, R. Gordon, S. R. de Cotret, N. Doiron-Leyraud, T. Saito, H. Fukazawa, Y. Kohori, K. Kihou, et al., Universal heat conduction in the iron arsenide superconductor kfe_2as_2: Evidence of a d-wave state, Physical Review Letters **109**, 087001 (2012).

[30] M. Abdel-Hafiez, V. Grinenko, S. Aswartham, I. Morozov, M. Roslova, O. Vakaliuk, S. Johnston, D. Efremov, J. Van Den Brink, H. Rosner, et al., Evidence of d-wave superconductivity in k 1- x na x fe 2 as 2 (x= 0, 0.1) single crystals from low-temperature specific-heat measurements, Physical Review B **87**, 180507 (2013).

[31] D. Wu, J. Jia, J. Yang, W. Hong, Y. Shu, T. Miao, H. Yan, H. Rong, P. Ai, X. Zhang, et al., Nodal $s_{\pm}$ pairing symmetry in an iron-based superconductor with only hole pockets, arXiv preprint arXiv:2212.03472 10.48550/arXiv.2212.03472 (2022).

[32] P. Richard, T. Sato, K. Nakayama, S. Souma, T. Takahashi, Y.-M. Xu, G. Chen, J. Luo, N. Wang, and H. Ding, Angle-resolved photoemission spectroscopy of the fe-based $ba_{0.6}k_{0.4}fe_2as_2$ high temperature superconductor: evidence for an orbital selective electron-mode coupling, Physical review letters **102**, 047003 (2009).

[33] Y. Cai, J. Huang, T. Miao, D. Wu, Q. Gao, C. Li, Y. Xu, J. Jia, Q. Wang, Y. Huang, G. Liu, F. Zhang, S. Zhang, F. Yang, Z. Wang, Q. Peng, Z. Xu, L. Zhao, and Z. X., Genuine electronic structure and superconducting gap structure in $(ba_{0.6}k_{0.4})fe_2as_2$ superconductor, Science Bulletin **66**, 1839 (2021).

[34] X. Luo, M. Tanatar, J.-P. Reid, H. Shakeripour, N. Doiron-Leyraud, N. Ni, S. L. Bud'ko, P. Canfield, H. Luo, Z. Wang, et al., Quasiparticle heat transport in single-crystalline $ba_{1-x}k_xfe_2as_2$: Evidence for a k-dependent superconducting gap without nodes, Physical Review B **80**, 140503 (2009).

[35] J.-P. Reid, M. Tanatar, X. Luo, H. Shakeripour, S. R. de Cotret, A. Juneau-Fecteau, J. Chang, B. Shen, H.-H. Wen, H. Kim, et al., Doping evolution of the superconducting gap structure in the underdoped iron arsenide $ba_{1-x}k_xfe_2as_2$ revealed by thermal conductivity, Physical Review B **93**, 214519 (2016).

[36] X. Hong, S. Sykora, F. Caglieris, M. Behnami, I. Morozov, S. Aswartham, V. Grinenko, K. Kihou, C.-H. Lee, B. Büchner, et al., Elastoresistivity of heavily hole-doped 122 iron pnictide superconductors, Frontiers in Physics **10**, 853717 (2022).

[37] A. Kuklov, N. Prokof'ev, and B. Svistunov, Commensurate two-component bosons in an optical lattice: Ground state phase diagram, Physical review letters **92**, 050402 (2004).

[38] A. Kuklov, N. Prokof'Ev, B. Svistunov, and M. Troyer, Deconfined criticality, runaway flow in the two-component scalar electrodynamics and weak first-order superfluid-solid transitions, Annals of Physics **321**, 1602 (2006).

[39] J. Garaud, M. Silaev, and E. Babaev, Thermoelectric signatures of time-reversal symmetry breaking states in multiband superconductors, Phys. Rev. Lett. **116**, 097002 (2016).

[40] J. Garaud and E. Babaev, Domain walls and their experimental signatures in s+ i s superconductors, Phys. Rev. Lett. **112**, 017003 (2014).